frontiers | Frontiers in Earth Science

TYPE Original Research
PUBLISHED 04 April 2024
DOI 10.3389/feart.2024.1387797

OPEN ACCESS

EDITED BY
Bin Gong,
Brunel University London, United Kingdom

REVIEWED BY
Pengfei Wang,
Taiyuan University of Technology, China
Zhaohui Wang,
China University of Mining and Technology, Beijing, China
Zhang Guangchao,
Shandong University of Science and Technology, China

*CORRESPONDENCE
Xidong Zhao,
xdz523@126.com

RECEIVED 18 February 2024
ACCEPTED 13 March 2024
PUBLISHED 04 April 2024

CITATION
Ma Z, Zhao X and Li S (2024), Mechanism of rockburst induced by roadway repair under intense mining: a case study.
Front. Earth Sci. 12:1387797.
doi: 10.3389/feart.2024.1387797

Mechanism of rockburst induced by roadway repair under intense mining: a case study

Zhenkai Ma[1], Xidong Zhao[2]* and Sheng Li[1]

[1]School of Mining, Liaoning Technical University, Fuxin, China, [2]School of Mine Safety, North China Institute of Science and Technology, Langfang, China

Rockbursts involve a sudden failure of the coal and rock mass without any apparent macroscopic precursors, threatening the production safety of coal mines. Achieving precise prediction of potential seismic body of rockbursts and determining their inducing factors are essential for effective prevention and control of rockbursts. By investigating the "1.17" major roof accident in the Danshuigou mine, the distribution characteristics of potential high-energy seismic body in the accident roadway during multi-layer mining were studied, relationship between these characteristics and the surrounding rock damage was established, and mechanism of the high-energy seismic body-induced rockbursts in the roadway was elucidated. It was found that the repair of the roadway floor was a key factor inducing the rockburst occurrence, with multi-layer mining generating potential high-energy seismic body reaching energy densities up to 10^6 J/m^3, resulting in roadway collapse and severe damage. Greater energy in these seismic body correlates with higher degrees of roadway impact damage. Moreover, higher energy accumulation in surrounding rock during roadway repairs leads to greater energy release. The triggering effects of roadway floor repair construction result in the instantaneous release of large elastic energy accumulated in ultrahigh-energy coal rock bodies, causing rock mass impact damage during triple mining. This study significantly contributes to understanding rockburst mechanisms and enhances the effectiveness of rockburst prediction and prevention.

KEYWORDS

strenuous mining activities, potential high-energy seismic body, roadway repair, energy release, rockburst

1 Introduction

Rockbursts, a type of mining pressure manifestation (Cai et al., 2020; Wang et al., 2020; Xuan et al., 2023), are major mining disasters (especially deep mining) that seriously threaten the production safety of coal mines (Dai et al., 2021; Dou et al., 2022; Pan et al., 2023). A rockburst is a dynamic disaster caused by the sudden release of energy accumulated in the rock surrounding a roadway or the surrounding coal and rock mass of a mining face (Jiang et al., 2023; Ma et al., 2023; Qi et al., 2023; Wu et al., 2023). Briefly, it is a sudden failure of the coal and rock mass that usually does not have apparent macroscopic precursors. When a rockburst occurs, coal and rock are suddenly ejected, causing a support breakage, coal wall collapse and roof fall, roadway blockage, and casualties accompanied by loud noises and rock mass vibrations

(He et al., 2016a; Liu et al., 2018; He et al., 2022). Possible mechanisms of rockburst-induced disasters have long been a focus of research studies. It is widely believed that the conditions for rockburst occurrence include a strength condition (the stress generated in the coal rock mass must exceed its strength of the coal rock mass to induce a coal rock mass failure), energy condition (the coal rock mass must continuously accumulate energy and be able to suddenly release it), and impact condition (the ability to undergo an impact failure) (Jiang et al., 2014; Dou et al., 2015; Liu et al., 2016; Liu et al., 2023).

Studying rock mechanics problems from the energy perspective has received increasing attention from the engineering and theoretical communities. Energy accumulation and release as the basic mechanical mechanisms of coal mine rockbursts have also become an important topic in the academic and engineering studies in recent years (Mazaira and Konicek, 2015; He et al., 2016b; He et al., 2018; He et al., 2021; Xue et al., 2021). Because the energy released in the surrounding rock during mining is the main cause of dynamic phenomena, exploring the accumulation and release of energy in the surrounding rock caused by mining should become the main research direction in the future and a new way of exploring the mechanism and prevention of rockburst disasters (Li et al., 2007; Xue et al., 2018; Du et al., 2022; Luo and Gong, 2023; Tang et al., 2023).

Zou and Jiang, (2004) applied the principle of energy transfer and law of energy conservation combined with an analysis of the weakening of rock mass characteristics and tissue damage to develop a theory of the impact effect in the coal rock mass. Wang et al. (2018) investigated the unstable energy triggering mechanism of rockbursts, identified the energy triggering conditions for dynamic disasters, and suggested rockburst prediction and prevention strategies. Wu et al. (2018) reported that the mining stress and accumulated energy carried by the external fault coal pillar of the working face continuously increased with an increase in the fault dip angle. Qi et al. (2019) constructed a theoretical and technical framework for the classification, protection, and governance of coal rock dynamic disasters at their sources. Shi et al. (2020) proposed a new rockburst classification method from the perspective of energy storage and release by considering the existing rockburst classification. Cao et al. (2022) suggested that the graben structure decreased the system stiffness, which in turn increased the energy storage level of the fault coal pillars inside the structure. Fu, (2023) performed theoretical calculations, numerical simulations, and laboratory tests to determine the impact kinetic energy and displacement potential energy released per unit area of the roadway on the 13230 working face of Gengcun Mine. Chen et al. (2023) studied the pre-peak energy of coal rock combinations and found that coal components were the main energy concentration regions.

Rockbursts are a special manifestation of the mine-induced earthquakes. The sudden fracture of a rock mass accompanied by a rockburst is a seismic event (Bieniawski et al., 1969; Hua and You, 2001; Zhou et al., 2018). In coal mining, identifying the potential seismic body of rockbursts and their key inducing factors are important prerequisites for achieving precise rockburst prevention and control. In this study, the "1.17" major roof accident in the Danshuigou coal mine is investigated to examine the distribution characteristics of a potential high-energy seismic body in the accident roadway during triple mining and establish their relationship with the surrounding rock damage of the rockburst roadway. In addition, a possible mechanism of the high-energy seismic body-induced roadway rockburst is proposed, which indicates that the repair of the roadway floor is a key inducing factor for the rockburst occurrence in the accident roadway. The obtained results have a wide range of engineering applications and can serve as a reference for achieving a better understanding the rockburst development process and improving the monitoring and prevention efficiency of rockburst disasters.

2 Project background

2.1 Project overview

On 17 January 2017, a major roof accident occurred in the Danshuigou coal mine located 15 km north of Shuocheng District, Shuozhou City, Shanxi Province. The accident occurred on the haulage roadway of the 4203 fully mechanized mining face, and the abnormal ground pressure generated by the accident was the first such event in this coal mine.

Five coal seams can be mined in Danshuigou Coal Mine, including coal seams 4-1, 4-2, 8, 9, and 11. First-level coal seams 4-1 and 4-2 are jointly arranged, and second-level coal seams 8, 9, and 11 are also jointly arranged. The 4203 fully mechanized working face is located to the north of the main roadway in coal seam 4, 4202 goaf is located to the east, and lower part of the 4202 goaf corresponds to the 9202 goaf in coal seam 9. The specific accident locations and onsite excavation engineering layouts are shown in Figure 1. The strike length of the working face 4203 is 1,091 m, dip length is 215 m, average thickness of the coal seam is 5.68 m, and average dip angle of the coal seam is 5°. The working face adopts a long-wall coal mining method, which is a comprehensive mechanized mining process, whereas a full caving method is used to manage the roof. The direct and main roofs of the working face are medium-coarse sandstone and mudstone, which represent undeveloped fissures. The thickness of the direct roof is 5.95 m, which belongs to the Class I stable roof category, and the thickness of the main roof is 3.97–9.04 m. The direct and old bottoms of the working face contain mudstone and fine sandstone, respectively, which represent undeveloped fissures. The thicknesses of the direct and old bottoms are 3.91–9.35 and 5.88 m, respectively. The 4203 haulage roadway is excavated along the floor of coal seam 4 with a rectangular cross-section. The roof support is a combination of bolts, anchor cables, steel belts, and metal diamond meshes.

2.2 Failure characteristics of the accident roadway

After a major roof accident occurred on the 4203 haulage roadway, the roadway started showing visible sectional damage and typical dynamic damage characteristics.

(1) The accident roadway exhibited apparent sectional damage characteristics. The 4203 haulage roadway was divided

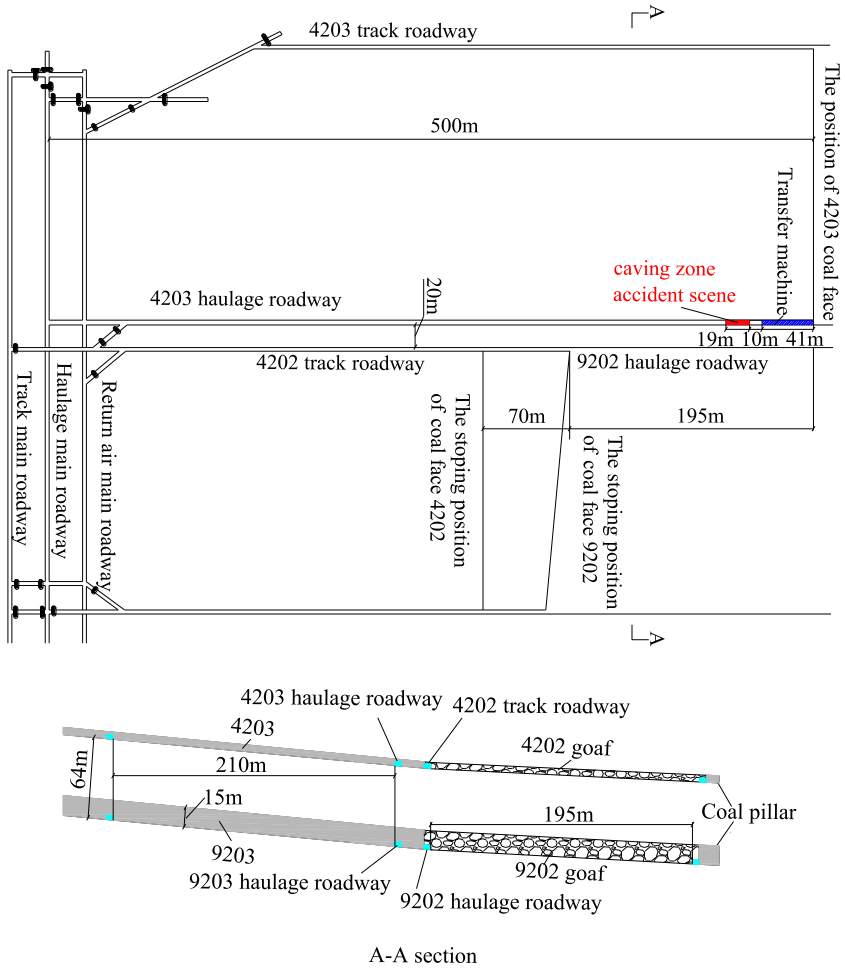

FIGURE 1
Schematic illustration of the accident location and surrounding mining layout of the 4203 working face haulage roadway.

into five sections from the end of the working face outwards, and their specific contents are described in detail in Table 1.

(2) The accident roadway demonstrated typical dynamic damage characteristics.

According to the accident investigation data, the steel wires of the deformation monitoring instruments for roadways 10, 9, and 8 located immediately in front of the roof collapse section, were broken (Figure 3), while the deformation monitoring instruments for the roadway in the normal area were intact. This phenomenon was rarely observed for non-dynamic roof-collapse accidents. The floor of the severely deformed section of the roadway exhibited typical dynamic characteristics, such as step bulging and extensive tilting, the tilting of the flatbed towards the solid side, and the dumping of materials on the vehicle. According to the data provided by the Center of Seismological Network of Shanxi Province, the SHC Shenchi Station (located ~42 km away), PIG Pianguan Station (located ~83 km away), KEL Kelan Station (located ~80 km away), and L1410 Yuanping Station (located ~78 km away) exhibited "earthquake anomalies" after the accident.

3 Establishment of a numerical model

3.1 Numerical calculation model

Based on the actual data obtained for the Danshuigou Mine, a numerical calculation model was developed (length × width × height = 1,000 m × 530 m × 170 m), where the horizontal displacements of the x-axis and y-axis boundaries and vertical displacement of the lower boundary of the z-axis were fixed (Figure 4). A compensation load of 8 MPa was applied to the upper boundary to simulate the unit weight of the rock layer above the model, and the initial stress field determined from the field stress data was applied. The Mohr–Coulomb constitutive model was used for calculations. The physical and mechanical properties of the rock masses are listed in Table 2.

To establish the relationship between the energy evolution in the surrounding rock of the 4203 haulage roadway and impact roof fall accident, the width and height of the 4203 haulage roadway were set to 5 × 4 m in the numerical calculation model. Considering the influence of roadway excavation on the stress change in the surrounding rock, the section size of the surrounding rock of the

TABLE 1 Descriptions of the sectional damage characteristics of the 4203 haulage roadway.

Serial number	Section Name	Section range	Description
I	Severe damage section at the end of the working face	0–41 m (as shown in Figure 1, length 41 m)	The transfer machine head was inclined with one side close to the roof and the other side located 350 mm away from the roof
II	Basic intact section of the roof	41–51 m (as shown in Figure 1, length 10 m)	The roof was basically intact
III	Impact roof collapse section	51–70 m (as shown in Figure 1, length 19 m)	The height of the roof collapse section reached the direct roof with a height of 2.0–2.5 m. Most anchor rods on the side were exposed, and the coal side collapsed (as shown in Figure 2)
IV	Damage section outside the roof collapse section	70–200 m	The 70–115 m section was damaged more severely. The roof and sides contained a net pocket, and the floor bulge was severe
V	Normal rock pressure manifestation section	200 m	The rock surrounding the roadway was basically intact

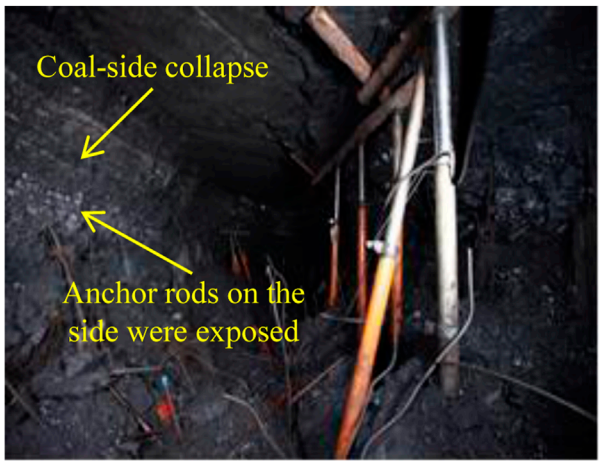

FIGURE 2
Photograph of the coal-side collapse.

4203 haulage roadway was set to 35 m × 26 m (width × height); that is, the ratio of the width direction to the roadway width was 7, and the height direction was 6.5. In this study, it was assumed that the rock mass outside the surrounding rock was not affected by roadway excavation.

3.2 Calculation schemes

Based on the mining layout of the working face during the 4203 haulage roadway roof fall accident in the Danshuigou Coal Mine, three different calculation schemes were proposed (Figure 5). Scheme A: Considering the influence of a single mining disturbance, only the 4203 working face was mined. Scheme B: Considering the influence of double mining disturbances, the 4202 working face was mined first to the stopping position, after which the 4203 working face was mined. Scheme C: Considering the influence of triple mining disturbances, the 4202 and 9202 faces were mined first to the stop-mining position followed by mining the 4203 face. In this model, the stopping positions for mining on the 4202, 9202, and 4203 working faces were Y = 755, 685, and 490 m, respectively. The horizontal distance between the 4203 working face and the 4202 and 9202 working faces were 265 m and 195 m, respectively.

4 Energy distribution characteristics of the rock surrounding the roadway

4.1 Energy accumulation characteristics of the rock surrounding the roadway

When the 4203 working face advanced to the accident location (Y = 490 m), the energy accumulated in the rock surrounding the mining roadway within the set section of the 4203 transportation roadway was calculated along the roadway axis with a length of 2 m used as the calculation unit (Figure 6). According to the calculation results, when the working face is not mined, the accumulated energy of the surrounding rock in the roadway remains unchanged at 1.31×10^7 J. In Schemes A and B, the energy accumulation in the surrounding rock of the roadway primarily occurs at distances of 40–150 m from the working face with peak values of 6.64×10^7 and 3.98×10^8 J, respectively. Scheme C shows that under triple mining conditions, the energy accumulated in the rock surrounding the roadway is much greater than the values calculated for single and double mining. The distribution characteristics of the accumulated energy in the rock surrounding the roadway exhibit first an increasing trend followed by a decreasing trend and stabilization. The energy accumulation process occurs up to a distance of 300 m

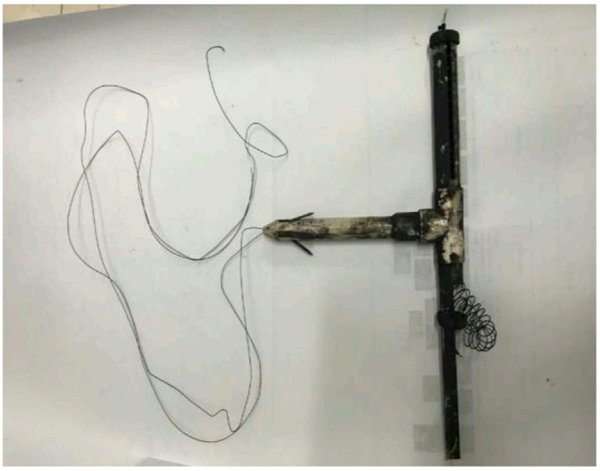

FIGURE 3
Photograph of the deformation monitoring instrument with steel wires cut off.

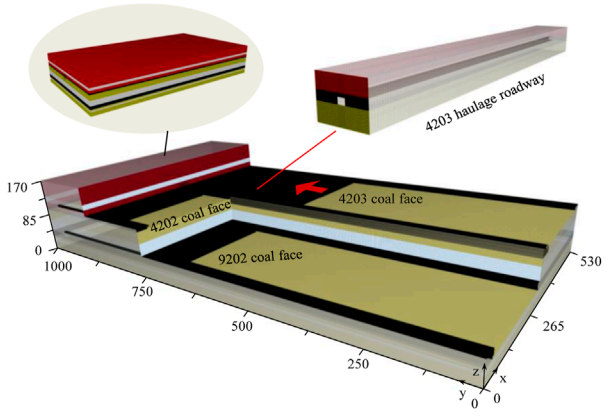

FIGURE 4
Numerical calculation model.

from the working face. The peak energy accumulated in the rock surrounding the roadway under the influence of triple mining can reach 9.78×10^8 J, which is 14.7 and 2.5 times greater than those obtained using Schemes A and B, respectively, and is 74.5 times higher than the energy accumulated in the rock surrounding the roadway without mining the working face.

According to the characteristics of the rockburst in the accident roadway, when the 4203 working face was mined to the accident location, the area where the abnormal rock pressure occurred in the roadway was located within a distance of 200 m from the working face, which was within the range of the energy accumulation in the rock surrounding the roadway. The severely damaged section (490–531 m) at the end of the accident roadway was located in the peak area of the energy accumulation in the rock surrounding the tunnel and its vicinity. The energy accumulated in the rock surrounding the roadway in this area was extremely high, 23.4–74.5 times greater than that of the non-mined working face. In the impact roof collapse section of the accident roadway (541–560 m), the accumulated energy of the rock surrounding the roadway is above 2.0×10^8 J; that is, the accumulated energy in this area is 16–20 times higher than that of the working face before mining. In the damaged section outside the roof collapse area of the accident roadway (560–690 m), the accumulated energy of the rock surrounding the roadway is above 8.52×10^7 J, which indicates that the accumulated energy value in this area is also more than 6.5 times greater than that of the working face before mining. Thus, under the influence of triple mining, the high-energy rock mass formed by the accumulation of a large amount of energy in the rock surrounding the roadway provides an energy basis for the occurrence of a rockburst.

4.2 Potential high-energy seismic body

To further explore the relationship between the energy distribution of the rock surrounding the roadway section and damaged state of the roadway, numerically calculated energy distributions of the surrounding rock were obtained for the different damaged sections of the 4203 haulage roadway using Scheme C and compared with the actual damaged state of the rock surrounding the roadway in different damaged sections when a rockburst occurred (Figure 7). According to the calculation data, in a high-stress environment generated under triple mining, the rock surrounding the roadway accumulates large amounts of energy and forms an ultrahigh-energy coal rock mass in local rock regions. When triggered by a certain event, a large amount of energy is instantly released, causing sudden damage to the surrounding rock, resulting in a rockburst accompanied by strong vibrations and loud noises. Therefore, this ultrahigh-energy coal rock mass is also a potential high-energy seismic body for rockburst formation. Potential high-energy seismic body is an ultrahigh-energy coal rock mass formed by highly concentrated surrounding rock energy in a high stress environment, and it is also the main energy body during the occurrence of rockburst. From a certain section of the roadway, the potential high-energy seismic body is located within a local area of the surrounding rock, and its energy density is tens or even hundreds of times higher than that of the original rock state. The positions of the potential high-energy seismic body and magnitude of the accumulated energy vary at different cross-sectional positions along the roadway axis. As the distance from the working face increases, the range and magnitude of the accumulated energy of the potential high-energy seismic body in different cross-sections gradually decrease.

In the severely damaged section at the end of the working face, the accumulation of energy in the rock surrounding the roadway is relatively high. At a distance of 20 m from the working face, the maximum energy density of the potential high-energy seismic body can reach 1.26×10^6 J/m^3, while the roadway cross-section in this section shrinks severely, individual hydraulic pillars are significantly bent, and most anchors and cables are damaged. In the basic intact section of the roof, the degree of energy accumulation in the rock surrounding the roadway decreases; however, the energy density of the potential high-energy seismic body in this section remains at a relatively high level. In the impact roof collapse section, the energy accumulation degree of the rock surrounding the roadway remains relatively high. At a distance of 55 m from the working face, the

TABLE 2 Mechanical properties of the stratified rock mass in the numerical model.

Stratum	Density/(kg/m^3)	Bulk Modulus/GPa	Shear Modulus/GPa	Cohesion/MPa	Friction Angle/°	Tensile Strength/MPa
Mudstone	2,480	5.97	2.85	4.4	32	1.1
Medium-coarse sandstone	2,630	9.50	7.20	13.0	38	2.2
Coal seam 4^{-2}	1,380	4.91	2.01	3.7	32	1.0
Fine sandstone	2,540	7.50	4.0	8.5	37	1.4
Mudstone	2,480	5.97	2.85	4.4	32	1.1
Coal seam 9	1,380	4.91	2.01	3.8	32	1.0
Mudstone	2,480	5.97	2.85	4.4	32	1.1
Fine sandstone	2,540	7.50	4.0	8.5	37	1.4

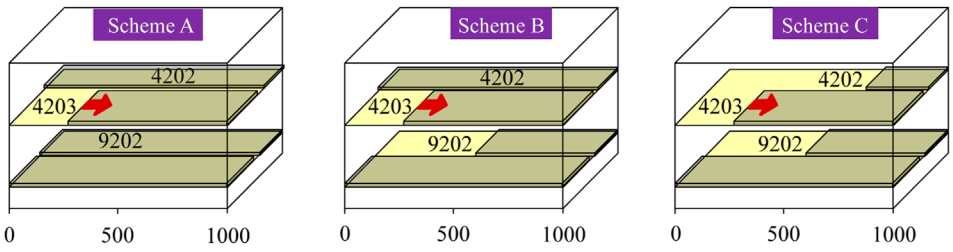

FIGURE 5
Mining layout schemes established for the working face. The red arrow represents extraction direction of 4203 working face.

maximum energy density of the potential high-energy seismic body is 6.47 × 10^5 J/m^3, roof caving height of the roadway in this section is 2.0–2.5 m, and collapsed roadway forms an arched trapezoid with apparent characteristics of the roof coal and roof stratification serving as the caving boundary. In the damaged section outside the collapsed roof, the degree of energy accumulation in the rock surrounding the roadway is further reduced. At a distance of 100 m from the working face, the maximum energy density of the potential high-energy seismic body is reduced to 3.78 × 10^5 J/m^3. Moreover, mesh pockets are present on the roof and sides of the roadway with severe bottom bulging, and the middle support leg of the belt conveyor is deformed and twisted. In the normal rock pressure manifestation section, at a distance of 250 m from the working face, the maximum energy density of the potential high-energy seismic body decreases to 8.95 × 10^4 J/m^3, while the deformations of the roof, floor, and two sides of the roadway in this section are insignificant, and the rock surrounding the roadway remains basically intact. By comparing the distribution characteristics of the potential high-energy seismic body with the degree of impact damage to the roadway, it is found that the greater the energy of the potential high-energy seismic body, the higher the impact damage degree to the roadway. However, the roof-collapse position of the roadway is not the location of the maximum potential high-energy seismic body. Therefore, it is necessary to further explore the energy release law of the surrounding rock during roadway repair.

5 Energy release laws of the rock surrounding the roadway

5.1 Energy release law of the rock surrounding the roadway established for different mining types

According to the calculation scheme designed earlier, for different mining layouts of the working face, when the 4203 working face advances to the accident location (Y = 490 m), a floor repair is performed along the roadway axis at the designated positions of the 4203 haulage roadway. The energy release values of the rock surrounding the mining roadway were calculated before and after the repair. Figure 8 shows the energy release values of the surrounding rock computed at different construction positions of the 4203 haulage roadway using the different mining schemes. The distribution of the energies released by the surrounding rock is the energy values released by the surrounding rock at different cross-sections after the repair of the roadway floor. After the repair of the roadway floor, the energy released by the surrounding rock roughly

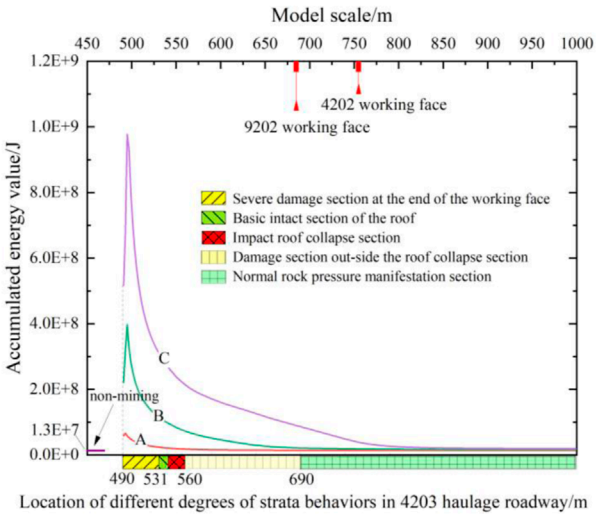

FIGURE 6
Distributions of the accumulated energy in the rock surrounding the roadway obtained using different mining schemes.

follows a normal distribution around the repair position, with its maximum value near the repair position and rapidly decreasing to a smaller value on both sides of the repair position. For the convenience of comparative research, it is generally centered around the repair location and a certain area is taken on both sides as the research interval. The energy release value of the surrounding rock within this area is the energy release interval value of the surrounding rock. The sum of the energy release interval values of the surrounding rock is the sum of the energy release values in the area with the largest energy released after repairing the roadway floor. The peak value of the energy released by the surrounding rock is the maximum energy released by the surrounding rock with different cross-sections after the repair of the roadway floor. The peak value of the energy released per unit volume of the surrounding rock is the maximum energy released per unit volume of the surrounding rock at different cross-sections after the repair of the roadway floor.

According to the calculation results, the energy released by the rock surrounding roadway is closely related to its energy state. The higher the accumulation degree of the energy field in the surrounding rock, the greater the amount of the released energy, which increases with the degree of mining influence. Taking the floor repair at a distance of 20 m (Y = 510 m) from the 4203 working face as an example, when only the 4203 working face is mined (Scheme A), the energy release value of the rock surrounding the roadway is smallest. Under the influence of dual mining (Scheme B), when the roadway floor is repaired, the total energy release interval, peak energy release interval, and peak energy release interval per unit volume are equal to 4.29×10^5, 1.33×10^5, and 1.08×10^4 J/m^3, respectively. Under the influence of triple mining (Scheme C), after repairing the floor, the total energy release interval of the rock surrounding the roadway can reach 2.29×10^6 J, which is 59.1, 27.4, and 5.4 times higher than those obtained for non-mining, single mining, and double mining in the working face, respectively. The peak value of the energy released by the rock surrounding the roadway is 6.03×10^5 J, which is 40.8, 19.6, and 4.5 times higher than the values obtained for non-mining, single mining, and double mining in the working face, respectively. The peak value of the energy release per unit volume of the surrounding rock is 3.14×10^4 J/m^3, which is 32.7, 12.3, and 2.9 times higher than those obtained for non-mining, single mining, and double mining in the working face, respectively.

5.2 Energy release law of the rock surrounding the roadway at different construction positions

According to the calculation results presented in Figure 8, when the floor repair construction is performed at different positions in front of the working face, the energy release value of the rock surrounding the roadway varies significantly. The overall trend shows that the released energy decreases with an increase in the distance from the working face, that is, with a decrease in the degree of mining influence. The accumulation level of the energy field in the surrounding rock is relatively low during mining in a single working face. Therefore, during the repair of the roadway floor, the overall energy release of the surrounding rock is low. Under the influence of dual mining, the energy released by the surrounding rock during the repair process of the roadway floor increases to a certain extent owing to the accumulation of the energy field in the rock surrounding the roadway. As the distance from the 4203 working face increases, the released energy approaches that of a single working face at a distance of 150 m (Y = 640 m) from the working face.

Owing to the strong influence of triple mining on the rock surrounding the roadway, the accumulation of the energy field in the surrounding rock is highest. Therefore, during the repair of the roadway floor, the energy released by the surrounding rock is also highest. As the distance from the 4203 working face increases, the energy release value at the designed position within a 100 m range of the working face is generally high; however, it exhibits a significant and rapid decrease. The decrease rate of the released energy value is gradually reduced at the position designed in the calculation scheme in the range of 100–300 m from the working face. After reaching the distance of 300 m from the working face, the released energy is close to the values obtained for single and double mining.

5.3 Energy release law of the rock surrounding the roadway at different mining positions

Under the influence of triple mining, when the 4203 working face is located at different mining positions, the released energy during the roadway repair process varies significantly owing to the different energy states of the surrounding rock of the 4203 haulage roadway. Taking the floor repair at a distance of 20 m from the 4203 working face as an example, the distribution of the energy released by the rock surrounding the 4203 haulage roadway and its interval

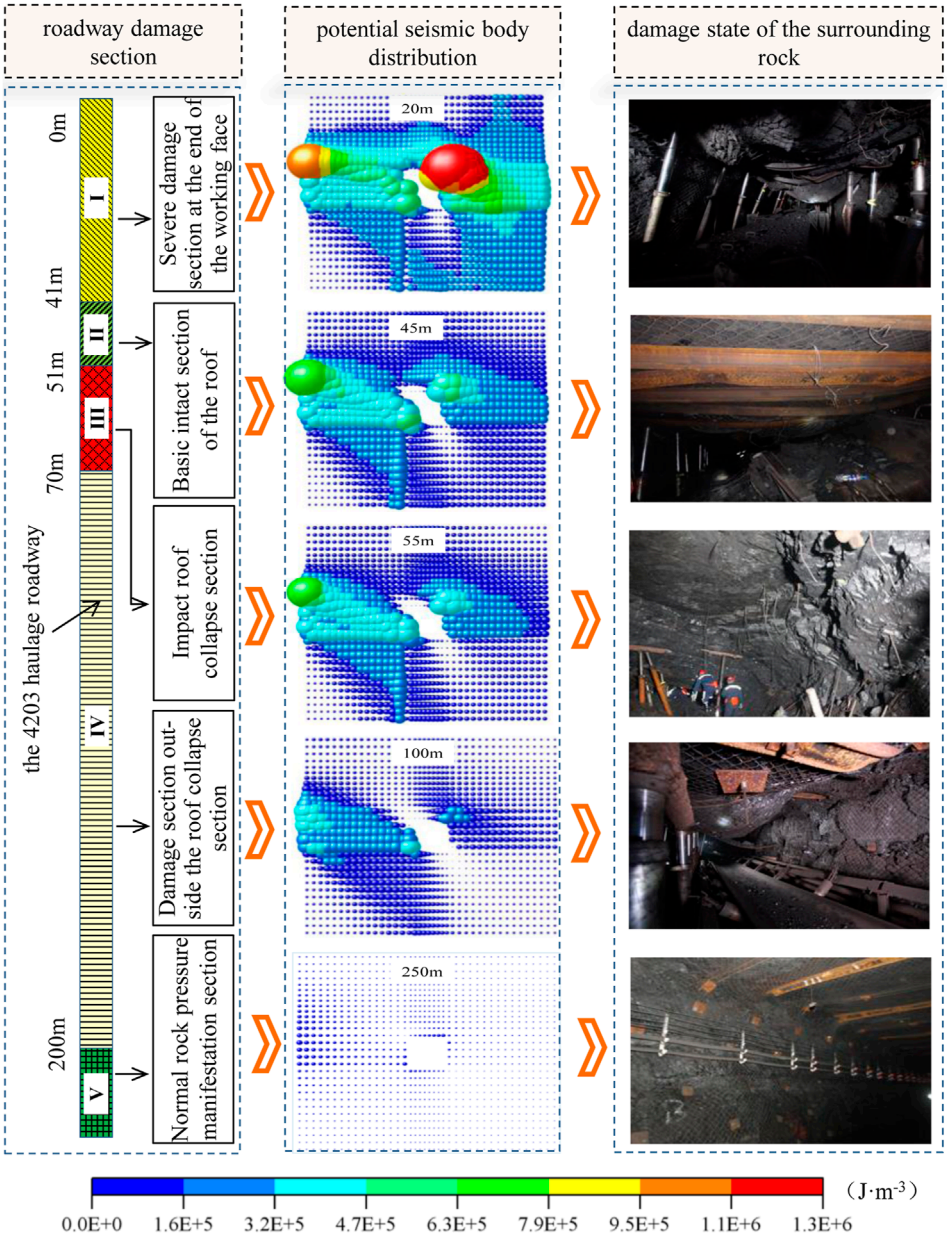

FIGURE 7
Potential high-energy seismic body versus the damage state of the surrounding rock.

peak obtained at different positions of the working face during triple mining are shown in Figure 9.

According to the calculation data, under the influence of triple mining, as the 4203 working face advances forward, the energy release value of the rock surrounding the roadway first increases, then decreases, increases again, and finally decreases. When the working face is located at different positions, consistent trends are obtained for the total energy release interval, peak energy release interval, and peak energy release interval per unit volume. When the 4203 working face advances from Y = 290 m to Y= 440 m, the energy released by the surrounding rock during the repair of the roadway floor exhibits a monotonic upward trend. Afterwards, as the 4203 working face continues to advance to Y= 640 m, the overall released energy value remains high despite the slight fluctuations. At Y = 640 m, the released energy reaches a peak value. During this process, the total energy release interval of the rock surrounding the roadway is (2.29–3.47) × 10^6 J, which is 59.1–89.5 times higher than the value obtained for the non-mined working face. The peak value of the energy released by the rock surrounding the roadway is (5.56–9.30) × 10^5 J, which is 37.6–62.9 times higher than that determined for the non-mined working face. The peak value of the energy release per unit volume of the rock surrounding the roadway is (2.79–5.61) × 10^4 J/m^3, which is 29.1–58.5 times higher than that obtained for the non-mined working face. Owing to the influence of the stopping positions of the 9202 (Y = 685 m) and 4202 (Y = 755 m) working faces, as the working face continues to advance, the released energy

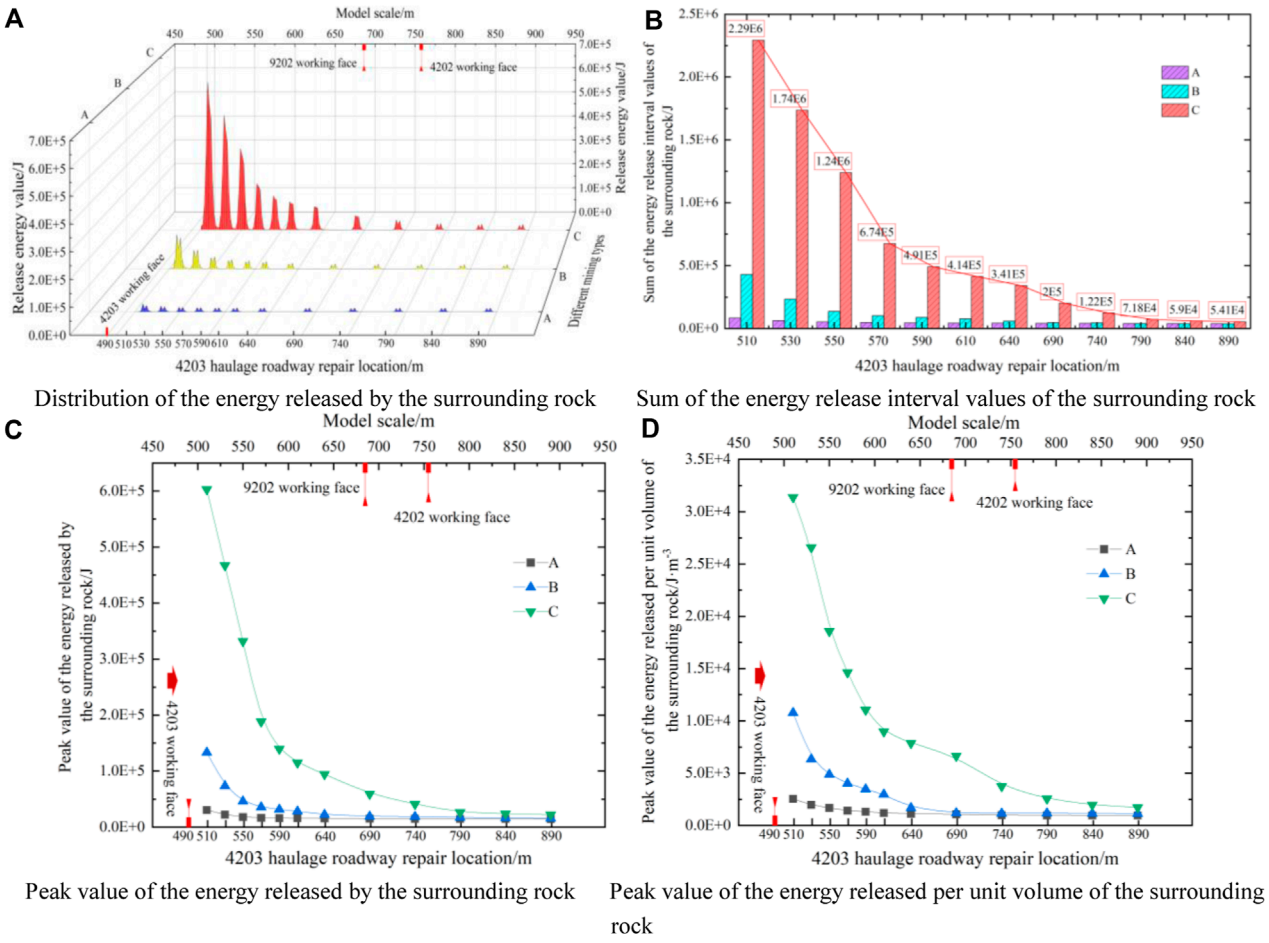

FIGURE 8
Energy release values of the surrounding rock determined at different construction positions of the 4203 haulage roadway and various mining schemes. **(A)** Distribution of the energy released by the surrounding rock. **(B)** Sum of the energy release interval values of the surrounding rock. **(C)** Peak value of the energy released by the surrounding rock. **(D)** Peak value of the energy released per unit volume of the surrounding rock.

begins to sharply decrease and gradually approaches the level of the original rock state.

5.4 Mechanism of the rockburst induced by roadway repair

Under the influence of triple mining, the rock surrounding the 4203 haulage roadway continuously accumulates energy and forms a high-energy storage rock mass, which in turn forms an ultrahigh-energy coal rock mass serving as a potential high-energy seismic body. During the mining process of the working face, with the dynamic changes in the stress field of the surrounding rock in the mining space, the degree of energy accumulation in the potential high-energy seismic body further increases. When the working face advances to the accident location, the repair construction of the roadway floor induces a rapid release of energy from the potential high-energy seismic body near the work area, which promotes the rapid adjustment of the surrounding rock stress field, at the same time, the stress waves formed by this process will also rapidly propagate in the rock mass and stimulate potential high-energy seismic body of different cross-sections to induce energy releases one by one. Owing to the extremely high propagation speed of the stress waves in the rock mass, the entire process of the energy release from different sections of the potential high-energy seismic body is also very fast, which is equivalent to the sudden release of the energy accumulated in the rock surrounding the roadway, thus forming a rockburst. Owing to the different cross-sections of the 4203 haulage roadway, the positions and energy magnitudes of the high-energy seismic body in the surrounding rock are different, resulting in segmented damage characteristics in the rockburst roadway.

6 Discussion

6.1 Mining period experienced by the rock surrounding the accident roadway

According to the relevant description of the accident process, when the rockburst occurred, the personnel trapped in the roof collapse section was repairing the roadway floor. Therefore, this section focuses on the floor repair as the rockburst-inducing factor

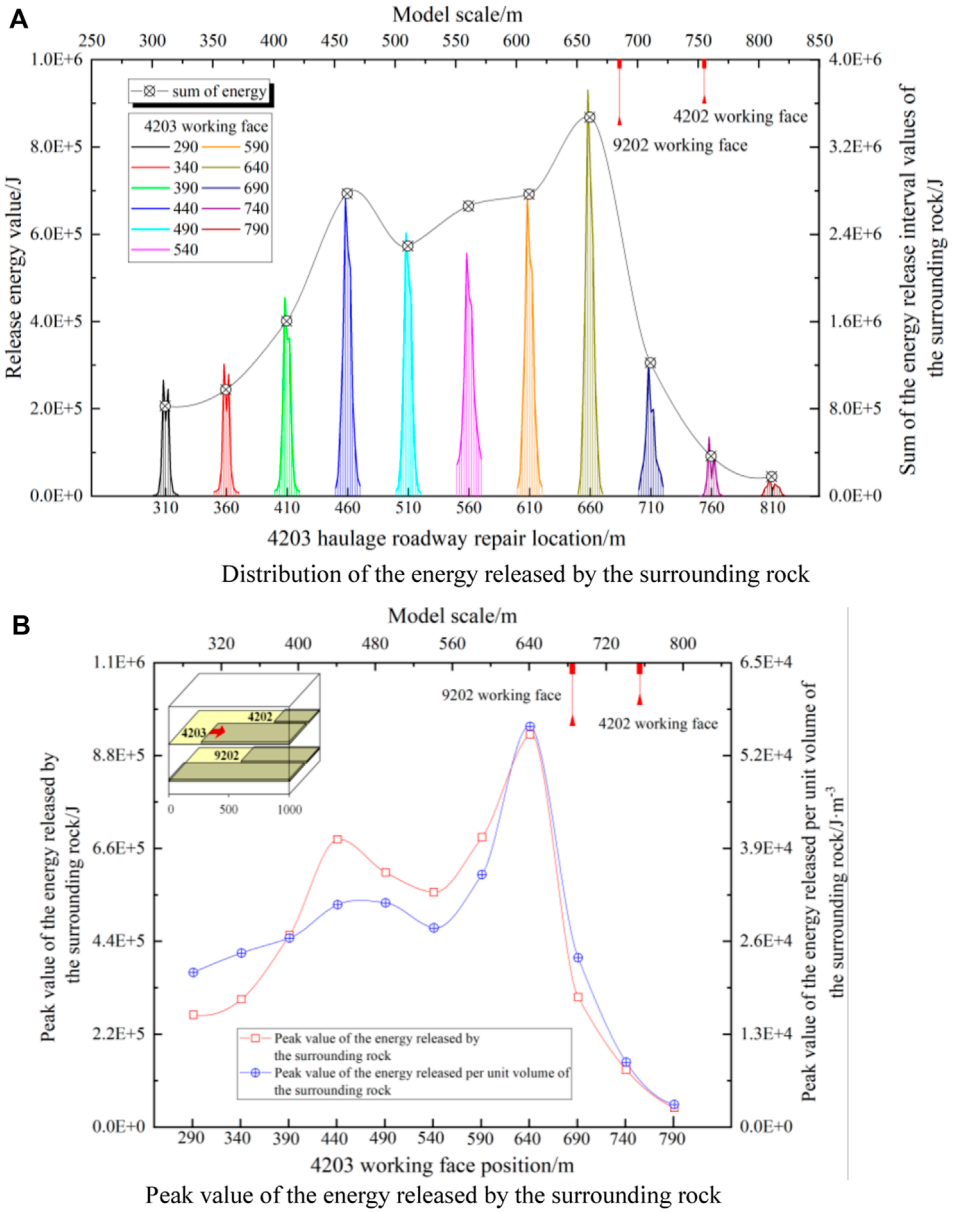

FIGURE 9
Energy release values of the surrounding rock in the 4203 haulage roadway obtained at different mining positions under the influence of multiple mining. **(A)** Distribution of the energy released by the surrounding rock. **(B)** Peak value of the energy released by the surrounding rock.

and adopts a time reversal verification method to discuss the rockburst occurred in the roadway during triple mining. From the beginning of excavation to the accident occurrence, the 4203 haulage roadway mainly went through the following four periods. 1) Non-mining period: the 4203 haulage roadway has completed excavation, working face has not been mined yet, and rock surrounding the roadway was not affected by the mining of the working face. 2) The first mining period: owing to the mining of the 4202 working face, the rock surrounding the roadway was only affected by the mining of a single working face. 3) Double mining period: after the cessation of mining of the 4202 working face, the mining of the 9202 working face was ongoing. 4) Triple mining period: based on the previous double mining process, the 4203 haulage roadway continued to be affected by the third mining of the 4203 working face. To examine the stress field and energy field evolution processes of the surrounding rock in the 4203 haulage roadway accident areas during different mining periods, a calculation scheme was designed based on the numerical model established earlier (Figure 10).

6.2 Force–energy evolution of the rock surrounding the accident roadway

The results obtained using the above-mentioned calculation scheme are presented in Figures 11–13. Figure 11 shows the calculation results obtained for the force-energy evolution process

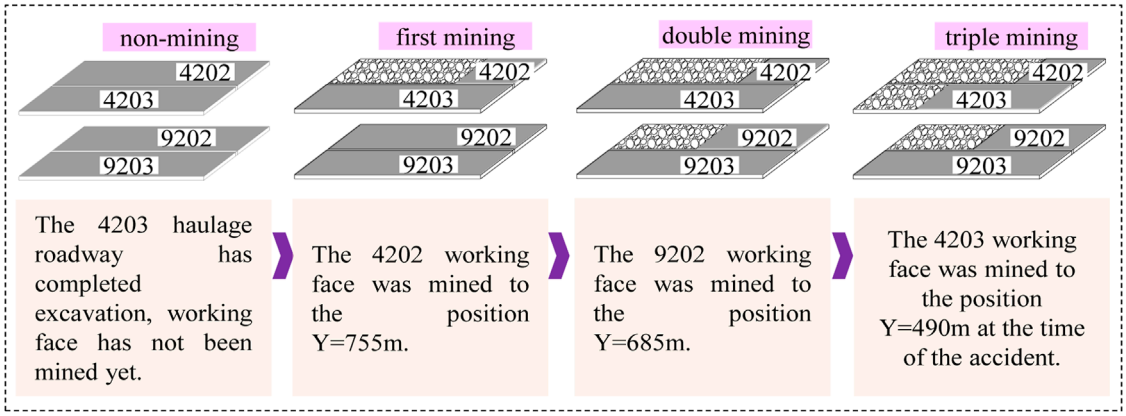

FIGURE 10
4203 haulage roadway during different mining periods.

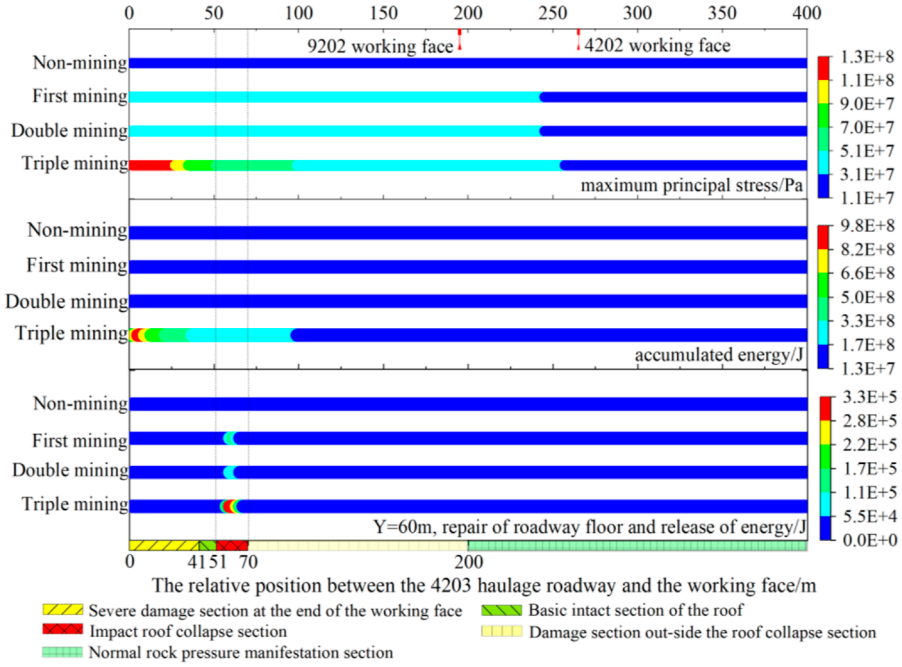

FIGURE 11
Force–energy evolution observed during different mining periods.

of the surrounding rock in the 4203 haulage roadway during the different mining periods. Figure 12 depicts the calculation results obtained for the force–energy evolution process of the surrounding rock in the impact roof collapse section of the 4203 haulage roadway during the different mining periods. The maximum principal stress is based on the centerline of the roof of the 4203 haulage roadway extracted along the roadway axis at a depth of 4 m. As the number of mining operations increases, the maximum principal stress of the surrounding rock during the different mining periods varies significantly. In particular, the maximum principal stress in the triple mining period is much higher than those in the other three periods, especially within the 70-m distance before the working face, and is up to 11.8 times higher than that obtained for the non-mining period. From the maximum principal stress of the surrounding rock in the impact roof collapse section, it can be concluded that as compared with the single mining period, the maximum principal stress value in the double mining period increases only slightly, and both values are approximately 4.3 times greater than that in the non-mining period, while the maximum principal stress value in the triple

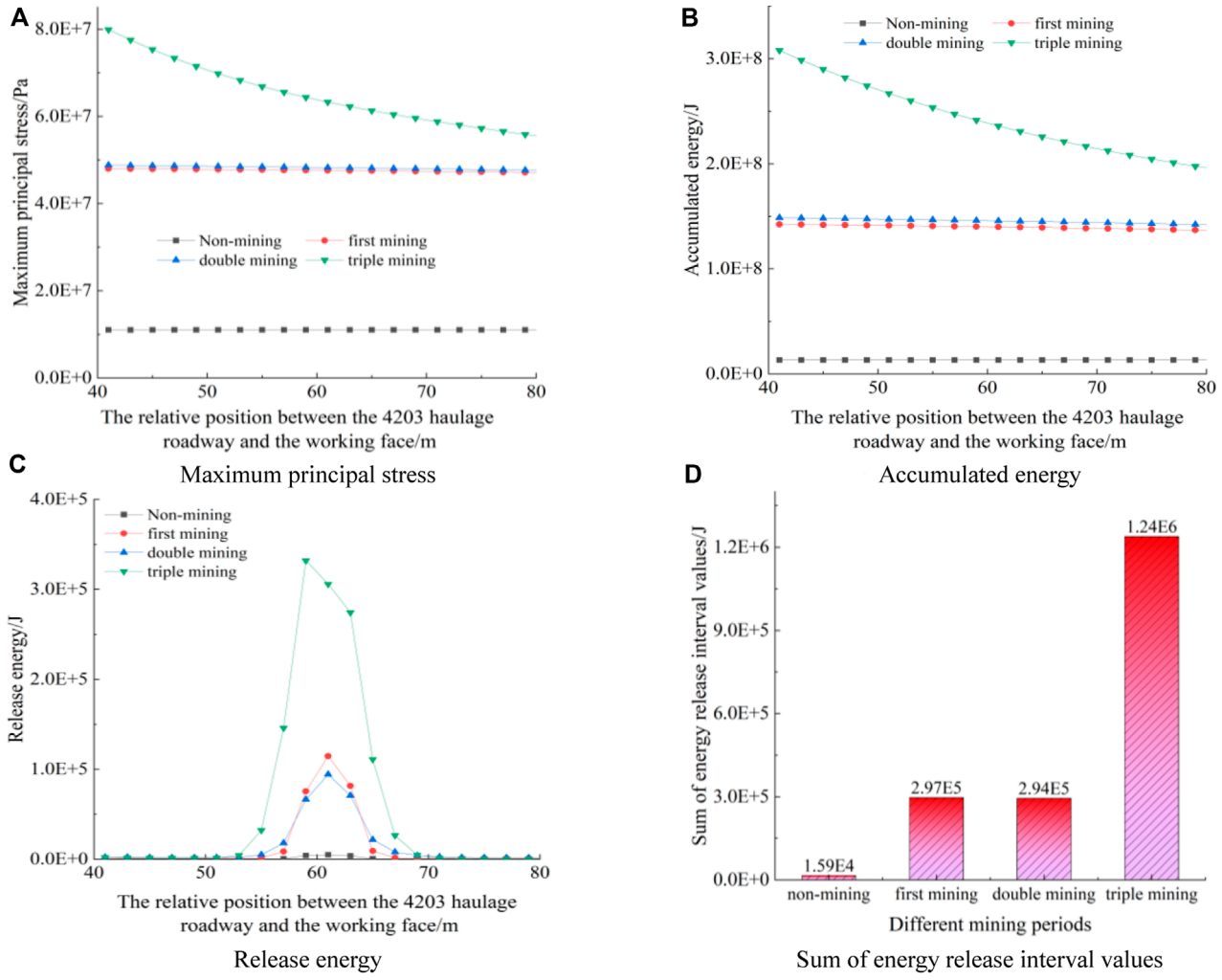

FIGURE 12
Force–energy evolution of the impacted roof collapse section observed during different mining periods. **(A)** Maximum principal stress. **(B)** Accumulated energy. **(C)** Release energy. **(D)** Sum of energy release interval values.

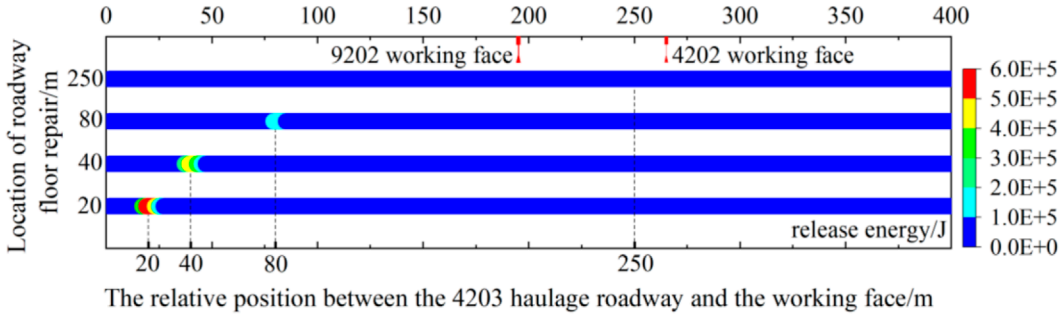

FIGURE 13
Energy release from the surrounding rock during floor repair at different roadway positions under the influence of triple mining.

mining period is 5.3–6.3 times higher than that obtained for the non-mining period.

According to the calculation results, during the triple mining period, the energy accumulated in the rock surrounding the roadway within a range of 70 m in front of the working face is much higher than the values obtained for the other three periods. The peak energy accumulated in the rock surrounding the roadway is 74.5 times higher than that of the non-mining period. The distribution

characteristics of the energy accumulated in the surrounding rock of the impact roof collapse section are similar to the maximum principal stress distribution. The observed increase in energy during the double mining period is not significant as compared with that during the single mining period, which is 10.5–11.2 times higher than the value obtained for the non-mining period. The energy accumulated in the surrounding rock during the triple mining period is 16.2–20.3 times higher than that accumulated during the non-mining period.

Based on the location of the personnel trapped in the roof collapse section during the repair operation of the roadway floor at the time of the accident, the repair position of the 4203 haulage roadway floor in the calculation model was set to Y = 550 m. By calculating the energy release value in the surrounding rock after the repair of the roadway floor during different mining periods, it can be concluded that as the number of mining operations increases, the stress and accumulated energy of the surrounding rock increase, and during the repair of the roadway floor, the energy released by the surrounding rock also increases. During the triple mining period, the peak range of the energy released by the surrounding rock reaches 3.3×10^5 J, which is 67.8, 2.9, and 3.5 times higher than those of the non-mining, single mining, and double mining periods, respectively. In the impact roof collapse section, the total interval of the energy released by the surrounding rock during the triple mining period is 1.24×10^6 J, which is 77.8, 4.2, and 4.2 times greater than those of the non-mining, single mining, and double mining periods, respectively. Therefore, the amount of energy released by the surrounding rock during roadway repair is directly related to the stress and accumulated energy in the surrounding rock. The higher the stress of the surrounding rock in the roadway, the higher the accumulated energy and the greater the energy released by the surrounding rock during roadway repair.

Based on the calculation results presented in Figure 13, the area of the energy release from the rock surrounding the roadway is strongly related to the floor repair location. The areas with high values of the released energy are concentrated within a certain range near the floor repair location; thus, a concentrated energy release occurs at the floor repair location. When repairing the floor of the roadway, the energy released by the surrounding rock increases with the number of mining operations. During the triple mining period, when the working face advances to the mining position at the time of the accident, the area of the energy release by the surrounding rock is concentrated within the front and back 20-m range centered at the repair position with a distance of 60 m from the working face, which is consistent with the range of the impact roof collapse section (51–70 m from the working face).

In summary, during the floor repair process, the repair location determines the primary release of energy from the rock surrounding the roadway. The magnitude of the stress concentrated in the surrounding rock and its accumulated energy determine the amount of energy released in the surrounding rock during the repair process. In other words, roadway repair is the key factor that triggers the release of a large amount of concentrated energy from the surrounding rock. In this process, the specific amount of energy released by the rock surrounding the roadway is determined by the energy accumulated in the surrounding rock.

6.3 Analysis of the induced rockburst during the accident roadway repair

During the triple mining period, the rock surrounding a certain roadway section in front of the working face accumulates a large amount of elastic energy in a high-stress environment; as a result, potential high-energy seismic body are formed in local areas. Owing to the repair operation of the roadway floor, a large amount of the elastic energy accumulated in the surrounding rock is instantly released, resulting in a sudden large-scale collapse of the roadway, which induces the breakage of all 19 roof anchor cables in the roof collapse area, and the breakage and bending of a large number of roof anchor bolts. Owing to the instantaneous release of energy from the surrounding rock and sudden rockburst occurrence, the floor repair workers and other workers located nearby were unable to anticipate the accident and evacuate in advance, resulting in the disaster. During the accident rescue process, nine victims of the roof collapse were located within the range of approximately 5 m who had no time to evacuate and run. Vibration sounds were still present during the on-site investigation after the accident. The detailed description and phenomenon of the accident further confirmed that the floor repair was the key cause of the rockburst.

7 Conclusion

This study analyzed the distribution characteristics of potential high-energy seismic body in accident roadways during triple mining, revealing their correlation with surrounding rock damage. Examination of a specific roadway section unveiled high-energy seismic body within localized rock formations with energy densities dozens to hundreds of times higher than the original rock. A constructed three-dimensional model illustrated that triple mining generated potential high-energy seismic sources reaching densities up to 10^6 J/m^3, leading to roof collapse and severe roadway damage. Comparison with roadway impact damage demonstrated a direct correlation between source energy and the degree of impact damage.

The energy release pattern of surrounding rock in the roadway was established, highlighting roadway floor repair as a key inducing factor for rockburst occurrence in accident roadways. During roadway repair, higher energy field accumulation in surrounding rock led to greater released energy values. The location of roadway repair determined concentrated energy release in surrounding rock, with stress magnitude and accumulated energy levels determining the extent of energy release during repair.

A potential mechanism of high-energy seismic body-induced rockburst occurrence on roadways was proposed. Under multi-layer mining influence, energy accumulation in surrounding rock generates potential high-energy seismic body locally. Triggered by roadway floor repair construction, instantaneous release of accumulated elastic energy in high-energy coal rock induces impact damage to the rock mass.

Data availability statement

The original contributions presented in the study are included in the article/supplementary material,

further inquiries can be directed to the corresponding author.

Author contributions

ZM: Conceptualization, Data curation, Formal Analysis, Investigation, Software, Validation, Visualization, Writing–original draft. XZ: Conceptualization, Data curation, Funding acquisition, Investigation, Project administration, Validation, Writing–review and editing. SL: Methodology, Resources, Supervision, Writing–review and editing.

Funding

The author(s) declare that financial support was received for the research, authorship, and/or publication of this article. This research was funded by the National Natural Science Foundation of China, grant number 51804117.

Acknowledgments

The authors would like to thank the peer reviewers and editors for their valuable comments and suggestions, which have greatly improved the manuscript presentation.

Conflict of interest

The authors declare that the research was conducted in the absence of any commercial or financial relationships that could be construed as a potential conflict of interest.

Publisher's note

References

Bieniawski, Z. T., Denkhaus, H. G., and Vogler, U. W. (1969). Failure of fractured rock. *Int. J. Rock Mech. Min. Sci. Geomech. Abstr.* 6, 323–341. doi:10.1016/0148-9062(69)90009-6

Cai, W., Bai, X., Si, G., Cao, W., Gong, S., and Dou, L. (2020). A monitoring investigation into rock burst mechanism based on the coupled theory of static and dynamic stresses. *Rock Mech. Rock Eng.* 53, 5451–5471. doi:10.1007/s00603-020-02237-6

Cao, A., Liu, Y., Jiang, S., Hu, Y., and Peng, Y. (2022). Occurrence mechanism and main control factors of coal burst near graben mining. *J. Min. Saf. Eng.* 39, 36–44+53. doi:10.13545/j.cnki.jmse.2021.0214

Chen, G., Li, T., Zhang, G., Li, J., Liu, G., He, Y., et al. (2023). Determination of bursting liability of coal-rock combined body based on residual energy release rate index. *Chin. J. Rock Mech. Eng.* 42, 1366–1383. doi:10.13722/j.cnki.jrme.2022.0882

Dai, L., Pan, Y., Li, Z., Wang, A., Xiao, Y., Liu, F., et al. (2021). Quantitative mechanism of roadway rockbursts in deep extra-thick coal seams: theory and case histories. *Tunn. Undergr. Space Technol.* 111, 103861. doi:10.1016/j.tust.2021.103861

Dou, L., He, J., Cao, A., Gong, S., and Cai, W. (2015). Rock burst prevention methods based on theory of dynamic and static combined load induced in coal mine. *J. China Coal Soc.* 40, 1469–1476. doi:10.13225/j.cnki.jccs.2014.1815

Dou, L., Tian, X., Cao, A., Gong, S., He, H., He, J., et al. (2022). Present situation and problems of coal mine rock burst prevention and control in China. *J. China Coal Soc.* 47, 152–171. doi:10.13225/j.cnki.jccs.yg21.1873

Du, F., Ma, J., Guo, X., Wang, T., Dong, X., Li, J., et al. (2022). Rockburst mechanism and the law of energy accumulation and release in mining roadway: a case study. *Int. J. Coal Sci. Technol.* 9, 67. doi:10.1007/s40789-022-00521-0

Fu, Y. (2023). Design method of support parameters for rock burst roadway based on energy calculation. *Coal Eng.* 55, 15–21. doi:10.11799/ce202312004

He, B., Zelig, R., Hatzor, Y. H., and Feng, X. (2016b). Rockburst generation in discontinuous rock masses. *Rock Mech. Rock Eng.* 49, 4103–4124. doi:10.1007/s00603-015-0906-8

He, J., Dou, L., Mu, Z., Cao, A., and Gong, S. (2016a). Numerical simulation study on hard-thick roof inducing rock burst in coal mine. *J. Cent. South Univ.* 23, 2314–2320. doi:10.1007/s11771-016-3289-4

He, M., Ren, F., and Liu, D. (2018). Rockburst mechanism research and its control. *Int. J. Min. Sci. Technol.* 28, 829–837. doi:10.1016/j.ijmst.2018.09.002

He, S., Song, D., Mitri, H., He, X., Chen, J., Li, Z., et al. (2021). Integrated rockburst early warning model based on fuzzy comprehensive evaluation method. *Int. J. Rock Mech. Min. Sci.* 142, 104767. doi:10.1016/j.ijrmms.2021.104767

He, Z., Lu, C., Zhang, X., Guo, Y., Meng, Z., and Xia, L. (2022). Numerical and field investigations of rock burst mechanisms triggered by thick-hard roof fracturing. *Rock Mech. Rock Eng.* 55, 6863–6886. doi:10.1007/s00603-022-03002-7

Hua, A., and You, M. (2001). Rock failure due to energy release during unloading and application to underground rockburst control. *Tunn. Undergr. Space Technol.* 16, 241–246. doi:10.1016/S0886-7798(01)00046-3

Jiang, F., Zhang, X., and Zhu, S. (2023). Discussion on key problems in prevention and control system of coal mine rock burst. *Coal Sci. Techno* 51, 203–213. doi:10.13199/j.cnki.cst.2022-1483

Jiang, Y., Pan, Y., Jiang, F., Dou, L., Ju, Y., Kaifi, J., et al. (2014). Phase I dose escalation study of capecitabine and erlotinib concurrent with radiation in locally advanced pancreatic cancer. *J. China Coal Soc.* 39, 205–210. doi:10.1007/s00280-014-2488-7

Li, X., Ma, N., Zhong, Y., and Gao, Q. (2007). Storage and release regular of elastic energy distribution in tight roof fracturing. *Chin. J. Rock Mech. Eng.* 26, 2786–2793.

Liu, G., Mu, Z., Chen, J., Yang, J., and Cao, J. (2018). Rock burst risk in an island longwall coal face by stress field. *Geosci. J.* 22, 609–622. doi:10.1007/s12303-017-0074-9

Liu, X., Tan, Y., Ning, J., Tian, C., and Tian, Z. (2016). Energy criterion of abutment pressure induced strain-mode rockburst. *Rock Soil Mech.* 37, 2929–2936. doi:10.16285/j.rsm.2016.10.026

Liu, X., Wang, G., Song, L., Bao, C., Wang, Z., Chang, Y., et al. (2023). Energy evolution in rockburst model under different gradient stress. *Int. J. Civ. Eng.* 21, 1495–1508. doi:10.1007/s40999-023-00834-4

Luo, S., and Gong, F. (2023). Evaluation of energy storage and release potentials of highly stressed rock pillar from rockburst control perspectives. *Int. J. Rock Mech. Min.* 163, 105324. doi:10.1016/j.ijrmms.2022.105324

Ma, Z., Li, S., and Zhao, X. (2023). Energy accumulation characteristics and induced rockburst mechanism of roadway surrounding rock under multiple mining disturbances: a case study. *sustainability* 15, 9595. doi:10.3390/su15129595

Mazaira, A., and Konicek, P. (2015). Intense rockburst impacts in deep underground construction and their prevention. *Can. Geotech. J.* 52, 1426–1439. doi:10.1139/cgj-2014-0359

Pan, Y., Song, Y., Zhu, C., Ren, H., and Xu, H. (2023). Localization method of coal rock deformation for rock burst prediction. *J. China Coal Soc.* 48, 185–198. doi:10.13225/j.cnki.jccs.2022.1375

Qi, Q., Li, Y., Zhao, S., Zhang, N., Zheng, W., Li, H., et al. (2019). Seventy years development of coal mine rockburst in China: establishment and consideration of theory and technology system. *Coal Sci. Techno* 47, 1–40. doi:10.13199/j.cnki.cst.2019.09.001

Qi, Q., Ma, S., Sun, X., Zhao, S., Li, Y., Li, H., et al. (2023). Theory and technical framework of coal mine rock burst origin prevention. *J. China Coal Soc.* 48, 1861–1874. doi:10.13225/j.cnki.jccs.2023.0158

Shi, T., Pan, Y., Wang, A., and Dai, L. (2020). Classification of rock burst in coal mine based on energy storage and release bodies. *J. China Coal Soc.* 45, 524–532. doi:10.13225/j.cnki.jccs.2019.0184

Tang, Z., Zuo, W., Lv, J., Yu, M., and Wu, Z. (2023). Study on factors influencing mechanical properties of energy absorbers for hydraulic support in rockburst roadway. *Int. J. Adv. Manuf. Technol.*, doi:10.1007/s00170-023-10852-0

Wang, G., Dou, L., Cai, W., Wang, Z., Gong, S., He, J., et al. (2018). Unstable energy triggering mechanism of rock burst. *J. China Univ. Min. Technol.* 47, 190–196. doi:10.13247/j.cnki.jcumt.000801

Wang, G., Li, G., Dou, L., Mu, Z., Gong, S., and Cai, W. (2020). Applicability of energy-absorbing support system for rockburst prevention in underground roadways. *Int. J. Rock Mech. Min.* 132, 104396. doi:10.1016/j.ijrmms.2020.104396

Wu, Q., Jiang, L., Kong, P., Wang, P., and Xu, C. (2018). Effects characteristics of fault pillar and its dip angle on mining-induced stress and energy distribution. *J. Min. Saf. Eng.* 35, 708–716. doi:10.13545/j.cnki.jmse.2018.04.007

Wu, S., Zhang, J., Song, Z., Fan, W., Zhang, Y., Dong, X., et al. (2023). Review of the development status of rock burst disaster prevention system in China. *J. Cent. South Univ.* 30, 3763–3789. doi:10.1007/s11771-023-5478-2

Xuan, Z., Cheng, Z., Li, C., Fan, C., Qin, H., Li, W., et al. (2023). Energy evolution mechanism during rockburst development in structures of surrounding rocks of deep rockburst-prone roadways in coal mines. *Front. Energy Res.* 11, 1283079. doi:10.3389/fenrg.2023.1283079

Xue, J., Du, X., Ma, Q., and Zhan, K. (2021). Experimental study on law of limit storage energy of rock under different confining pressures. *Arab. J. Geosci.* 14, 62–68. doi:10.1007/s12517-020-06398-0

Xue, Y., Cao, Z., Du, F., and Zhu, L. (2018). The influence of the backfilling roadway driving sequence on the rockburst risk of a coal pillar based on an energy density criterion. *Sustainability* 10, 2609.doi:10.3390/su10082609

Zhou, J., Li, X., and Mitri, H. (2018). Evaluation method of rockburst: state-of-the-art literature review. *Tunn. Undergr. Space Technol.* 81, 632–659. doi:10.1016/j.tust.2018.08.029

Zou, D., and Jiang, F. (2004). Research of energy storing and gestation mechanism and forecasting of rockburst in the coal and rock mas. *J. China Coal Soc.* 29, 33–37. doi:10.13225/j.cnki.jccs.2004.02.008